

Unusual Pressure-Induced Quantum Phase Transition from Superconducting to Charge-Density Wave State in Rare-Earth-Based Heusler LuPd₂In Compound

Heejung Kim,^{1,2} J. H. Shim^{1,3} , Sooran Kim,⁴ Jae-Hoon Park^{1,2,6} , Kyoo Kim^{1,2,5,*} , and B. I. Min^{1,†} 

¹Department of Physics, POSTECH, Pohang 37673, Korea

²MPPHC-CPM, Max Planck POSTECH/Korea Research Initiative, Pohang 37673, Korea

³Department of Chemistry, POSTECH, Pohang 37673, Korea

⁴Department of Physics Education, Kyungpook National University, Daegu 41566, Korea

⁵Korea Atomic Energy Research Institute (KAERI), 111 Daedeok-daero, Daejeon 34057, Korea

⁶Division of Advanced Materials Science, POSTECH, Pohang 37673, Korea

 (Received 29 July 2019; revised 10 March 2020; accepted 10 September 2020; published 5 October 2020)

We investigate the pressure effects on the electronic structures and phonon properties of rare-earth-based cubic-Heusler compound LuPd₂In, on the basis of *ab initio* density functional theory. We find the occurrence of intriguing phase transition from the superconducting (SC) to charge-density wave (CDW) state under pressure (*P*), which is quite unusual in that the pressure is detrimental to the CDW state in usual systems. The SC transition temperature T_C of LuPd₂In increases first with increasing pressure, up to $P_C \approx 28$ GPa, above which a quantum phase transition into the CDW state takes place. This extraordinary transition originates from the occurrence of phonon softening instability at a special $\mathbf{q} = M$ in the Brillouin zone. We thus propose that LuPd₂In is a quite unique material, in which the CDW quantum critical point is realized under the SC dome by applying the pressure.

DOI: 10.1103/PhysRevLett.125.157001

The competition between superconductivity and charge-density wave (CDW) state has been studied during the last half-century in various materials of different structures. The typical examples include A15 compounds [1,2], A₃T₄Sn₁₃ (A = La, Sr, Ca, T = Ir, Rh) [3–6], and transition-metal dichalcogenides such as IrTe₂ [7], AuTe₂ [7–10], 2H-TaS₂, 2H-TaSe₂ [11], and 1T-TiSe₂ [12]. Despite the diversity in materials, all the above compounds exhibit the common phase diagram, as depicted in Fig. 1(a). Those materials exhibit the CDW phases with the pronounced peak structures in the Lindhard susceptibilities of the parent compounds. In general, with tuning parameters, such as doping, intercalation, and pressure, the CDW phase gets destabilized with diminished CDW transition-temperature (T_{CDW}), and then the superconductivity is developed at low temperature (*T*) due to the enhanced electron-phonon coupling, as shown in Fig. 1(a). When T_{CDW} decreases continuously down to zero at the point of a certain parameter value, we call such point a CDW quantum-critical point (QCP). As shown in Fig. 1(b), Lu(Pt_{1-x}Pd_x)₂In of present interest shows a superconducting (SC) dome with the maximum T_C at the QCP. Although the magnetic QCP has been frequently reported near the vanishing point of magnetic order in heavy fermions [13–15], iron pnictides [16–21], and high- T_C cuprates [22–26], the direct observation of the CDW QCP has been rare. The CDW QCP has been only recently identified in A₃T₄Sn₁₃ [3–6] and *o*-TaS₃ [27] by increasing pressure or intercalation. The rare-earth-based full-Heusler

compound Lu(Pt_{1-x}Pd_x)₂In has also been studied as a candidate of a CDW QCP system by Gruner *et al.* [28]. As shown in Fig. 1(b), LuPt₂In exhibits the CDW transition at $T_{CDW} = 490$ K, and the substitution of Pd for Pt induces the linear decrease of T_{CDW} toward zero with the destabilization of CDW. Interestingly, even before T_{CDW} becomes zero, the emergent superconductivity coexists at low *T* inside the CDW state of Lu(Pt_{1-x}Pd_x)₂In, where T_C increases with Pd substitution. Then the T_C has a maximum value (1.10 K) at the CDW QCP with $x = 0.58$ of Pd substitution, where T_{CDW} becomes zero. The next natural question is how the pressure affects the SC properties in Lu(Pt_{1-x}Pd_x)₂In. LuPd₂In is also a superconductor with T_C less than 0.35 K [28]. It is tempting to expect that the pressure will enhance the T_C of LuPd₂In.

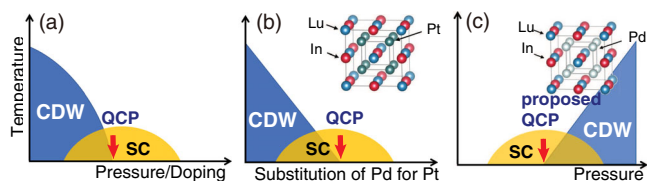


FIG. 1. (a) A common $T - P$ (or *doping*) phase diagram of typical CDW-SC competing materials. (b) The observed T vs Pd-substitution phase diagram for Lu(Pt_{1-x}Pd_x)₂In [28]. (c) A schematic $T - P$ phase diagram of LuPd₂In. QCPs are denoted by red arrows. For all three cases, CDW and SC states coexist in their overlapped regime. Insets of (b) and (c) show the crystal structures of LuPt₂In and LuPd₂In, respectively.

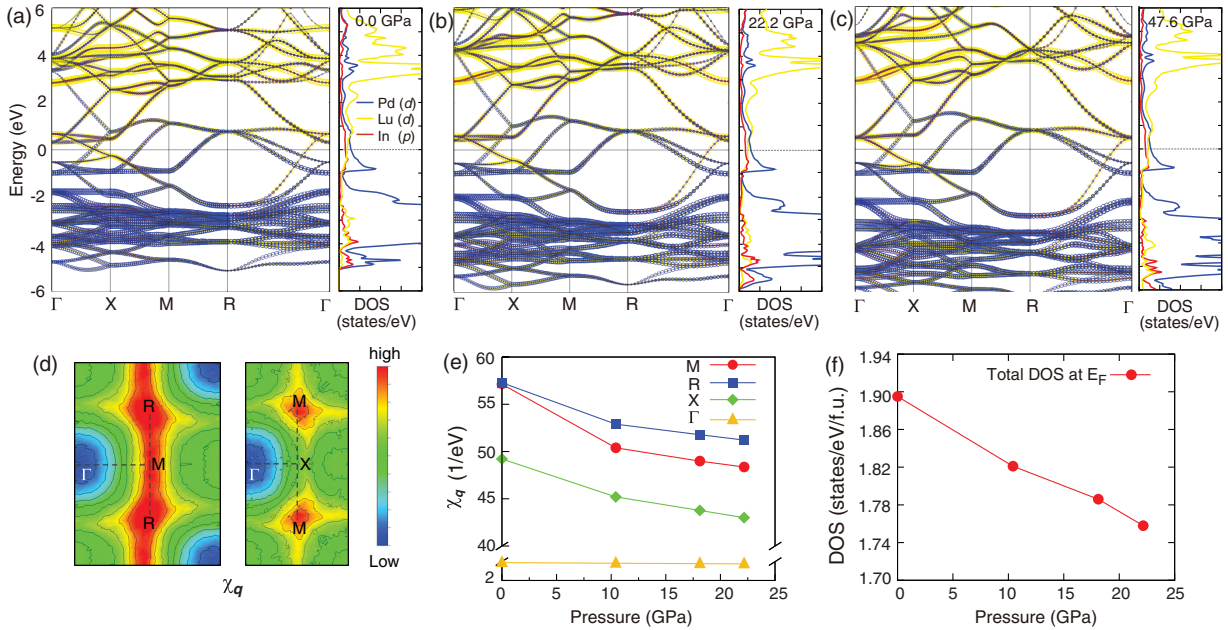


FIG. 2. (a)–(c) Band structures and DOS of LuPd₂In for different pressures. Bands are plotted along the symmetry lines of the cubic BZ. (d) The contour plots of real part of charge susceptibility χ_q of LuPd₂In at the ambient pressure. (e),(f) The behaviors of χ_q and the total DOS at E_F with increasing pressure.

In this Letter, we have investigated the pressure effects on the electronic structures and phonon properties of LuPd₂In, employing density-functional theory (DFT) calculations. We have observed an extraordinary phonon softening anomaly at $\mathbf{q} = M$ in LuPd₂In under pressure. In consequence, T_C of LuPd₂In becomes enhanced with increasing pressure, up to 1.36 K at the QCP, at which the softened phonon eventually has an imaginary frequency, suggesting the CDW instability. We have clearly shown that the phonon softening instability indeed originates from the enhanced electron-ion deformation potential under pressure. In this way, we have demonstrated that unusual pressure-induced quantum phase transition to a CDW state can be realized with the QCP under the SC dome in LuPd₂In, as depicted in Fig. 1(c), which is quite distinct from other typical CDW-SC competing materials shown in Fig. 1(a). We predict that a maximum T_C can be attained for LuPd₂In at the QCP of $P_C \approx 28$ GPa.

Band structures and susceptibilities were obtained by employing the full-potential band method implemented in the WIEN2k package [29]. Phonon dispersions and electron-phonon coupling (EPC) constants were obtained by using the density-functional perturbation theory [30] implemented in the QUANTUM ESPRESSO package [31]. Computational details are provided in the Supplemental Material [32].

Figures 2(a)–2(c) show the band structures of LuPd₂In along the symmetry lines of the cubic Brillouin zone (BZ) of conventional unit cell [see Fig. S2(h) in the Supplemental Material [32]] for different pressures. Pd $4d$ states mainly contribute to the bands near the Fermi

level (E_F) for the considered pressure range. While the overall bandwidths including conduction and valence bands increase with increasing pressure, the bandwidths near E_F increase only slightly. Also, the shapes of the band structures near E_F are almost unchanged under pressure, which indicates the invariance of the Fermi surface (FS) topology.

To investigate the electronic instability, we have calculated the real part of charge susceptibility (χ_q) with changing pressure. As shown in Fig. 2(d), at the ambient pressure, the pronounced χ_q peaks are located along M – R , signifying the existence of the possible electronic instabilities along those \mathbf{q} lines. This feature is sustained under the variation of pressure, as shown in Fig. 2(e). But the intensity of χ_q at each \mathbf{q} is reduced with increasing pressure, as the behavior of the density of states (DOS) at E_F in Fig. 2(f). The decrease of susceptibility appears to suggest that the structural instability becomes weakened with increasing pressure, as in typical CDW systems of Fig. 1(a), which, however, turns out to be not true for LuPd₂In.

To investigate the phonon and SC properties of LuPd₂In, we have calculated the phonon dispersion, phonon density of states (PDOS), Eliashberg spectral function [$\alpha^2F(\omega)$], and the EPC constant ($\lambda_{q\nu}$) with varying pressure, as provided in Fig. 3. The magnitude of $\lambda_{q\nu}$ is represented by the color in the phonon dispersion curve in Fig. 3(a). At the ambient pressure, the contributions from all the atoms to the PDOS are more or less similar in the low-frequency region (below 8 meV) with a slightly larger value from Pd. The contribution of the lightest element (In) is dominating in the

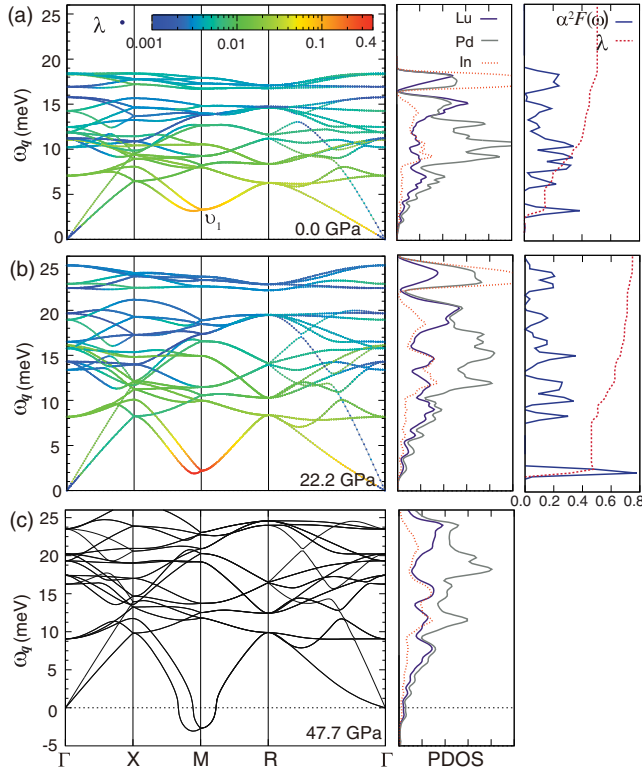


FIG. 3. The phonon dispersion with $\lambda_{\mathbf{q}\nu}$, PDOS, and $\alpha^2 F(\omega)$ at (a) the ambient pressure, (b) 22.2 GPa, and (c) 47.7 GPa. The negative frequency means the imaginary value of the softened phonon frequency. The color in the phonon dispersion represents the magnitude of $\lambda_{\mathbf{q}\nu}$.

high-frequency region (16–20 meV), while the contribution of Lu is prevalent in the overall frequency range.

It is notable in Fig. 3(a) that the lowest-energy normal mode (ν_1) at $\mathbf{q} = M$, having fourfold degeneracy, shows the phonon softening anomaly. Another prominent feature is that $\lambda_{M\nu_1}$ is much larger than other $\lambda_{\mathbf{q}\nu}$'s by 10 times. This indicates that $\lambda_{\mathbf{q}\nu}$ at $\mathbf{q} = M$ is distinctively large. Accordingly, the total EPC constant $\lambda_{\text{tot}} (= 0.506)$ is contributed mainly from $\lambda_{M\nu_1}$. Utilizing McMillan's formula, shown in the Supplemental Material [32], we obtain $T_C = 0.45$ K for LuPd₂In at the ambient pressure, as is consistent with the experimental result [28].

Under pressure, phonons tend to be hardened due to the increment of the bond strength between ions. Indeed, for LuPd₂In, the overall phonon dispersions at 22.2 and 47.7 GPa in Figs. 3(b) and 3(c) become more hardened than that at the ambient pressure, manifesting the widespread PDOS in Figs. 3(b) and 3(c). By contrast, the phonon frequency at M , having the largest λ , becomes softened with increasing pressure. Figure 4(a) shows the evolution of the frequency of the ν_1 ($\mathbf{q} = M$) mode under pressure. We have observed that it becomes imaginary at $P \approx 28$ GPa, signifying the CDW structural instability. This result indicates that LuPd₂In having the non-CDW SC ground state at the ambient pressure will experience the CDW transition with increasing pressure, as shown in the phase diagram of Fig. 1(c). Furthermore, this suggests that $P \approx 28$ GPa would be the QCP in pressurized LuPd₂In, at which T_C would have a maximum value.

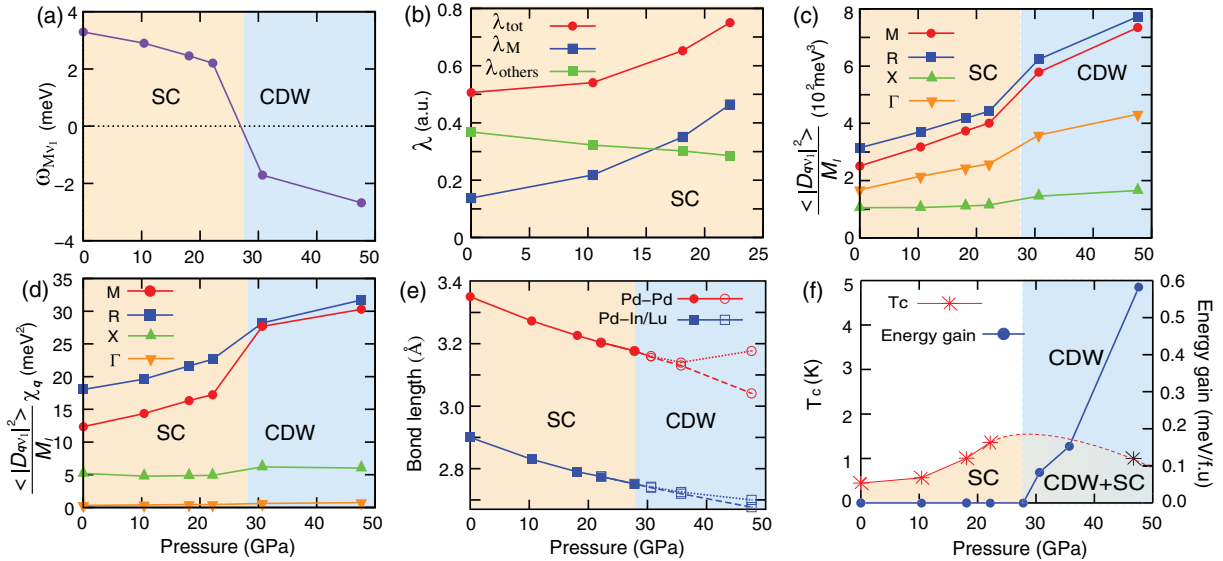


FIG. 4. Physical variables as a function of pressure in LuPd₂In. (a),(b) The phonon frequency ($\omega_{M\nu_1}$), λ_M , λ_{others} , and λ_{tot} . (c),(d) $\langle |D_{\mathbf{q}\nu_1}|^2 \rangle / M_I$ and $\langle |D_{\mathbf{q}\nu_1}|^2 \rangle \chi_{\mathbf{q}} / M_I$ in Eq. (1) for the lowest-energy ν_1 optical mode at different \mathbf{q} 's. (e) The variation of bond lengths. The bond lengths are split in the CDW state, and so the splitting size can be taken as the CDW order parameter. (f) SC T_C and the energy gain of CDW phase with respect to non-CDW phase. The black star denotes the estimated T_C in the CDW phase.

We have also checked the variation of $\lambda_{\mathbf{q}\nu}$ with increasing pressure in Fig. 4(b). All the $\lambda_{\mathbf{q}\nu}$'s go down with pressure except for $\lambda_{M\nu_1}$. Hence, despite the suppression of other $\lambda_{\mathbf{q}\nu}$'s, the increment of the $\lambda_{M\nu_1}$ brings about an eventual increase of λ_{tot} with increasing pressure, which yields the enhancement of T_C up to 1.37 K at 22.2 GPa, as shown in Fig. 4(f).

Our finding reveals that T_C of Lu(Pt_{1-x}Pd_x)₂In can be enhanced not only by substitution of Pd [28] but also with increasing pressure. Moreover, LuPd₂In experiences the abnormal pressure-induced phase transition from SC to CDW state with the emergence of quantum criticality. The pressure-induced CDW transitions were also observed in some semiconducting systems like SnSe₂ [41]. For SnSe₂, it happens because a newly developed FS due to applied pressure has either the high DOS at E_F or the nesting feature. However, LuPd₂In under pressure shows neither the high DOS at E_F nor the change in the FS topology, as shown in Figs. 2(e) and 2(f). Therefore the pressure-induced CDW transition observed in LuPd₂In is quite unusual in metallic systems.

Now we address the questions of why only $\lambda_{M\nu_1}$ increases with pressure and why the abnormal transition takes place in pressurized LuPd₂In, in spite of the reduction of $\chi_{\mathbf{q}}$ and DOS at E_F . In the McMillan-Hopfield formula [34,35], λ_{tot} can be expressed as $\lambda_{\text{tot}} = \{[N(E_F)]/[\langle\omega^2\rangle]\} \{[\langle|D|^2\rangle]/[M_I]\}$, where $N(E_F)$ is the total DOS at E_F , $\langle|D|^2\rangle$ is the averaged deformation-potential square, M_I is the ionic mass, and $\langle\omega^2\rangle$ is the averaged phonon-frequency square. Here, the deformation-potential D is defined as the derivative of electron-ion interaction with respect to ion displacement [32]. Because the main contribution of λ_{tot} comes from $\lambda_{M\nu_1}$, one can approximate the value by $\lambda_{\text{tot}} \approx [N(E_F)/\langle\omega_{M\nu_1}^2\rangle] [\langle|D_{M\nu_1}|^2\rangle/M_I]$. So far, the magnitude of deformation-potential $D_{\mathbf{q}\nu}$ has been checked only indirectly by comparing the band splitting near E_F between the original and the distorted structure induced by the corresponding normal mode. Here, we measured $\langle|D_{\mathbf{q}\nu}|^2\rangle$ for each \mathbf{q} and ν directly from the phonon linewidth $\gamma_{\mathbf{q}\nu}$. Namely, as described in the Supplemental Material [32], the average value of $\langle|D_{\mathbf{q}\nu}|^2\rangle/M_I$ is related to $\gamma_{\mathbf{q}\nu}$. Figure 4(c) provides the evaluated $\langle|D_{\mathbf{q}\nu}|^2\rangle/M_I$ values for ν optical mode at each \mathbf{q} for different pressures. As expected, the $\langle|D_{\mathbf{q}\nu}|^2\rangle/M_I$ values are enhanced with pressure due to the increase of bonding strength. It is worth noting that the increasing rates of $\langle|D_{\mathbf{q}\nu}|^2\rangle/M_I$ with pressure at $\mathbf{q} = M$ and R are much larger than those at X and Γ . This implies that the EPC term in LuPd₂In is strengthened at both M and R under pressure. The increasing $\langle|D_{\mathbf{q}\nu}|^2\rangle/M_I$ with pressure will enhance $\lambda_{\mathbf{q}\nu}$, but the decreasing $N(E_F)$ in Fig. 2(f) and the increasing $\omega_{\mathbf{q}\nu}$ ($\mathbf{q} \neq M$) in Fig. 3 with pressure will reduce $\lambda_{\mathbf{q}\nu}$. As a consequence of two opposite contributions, all the $\lambda_{\mathbf{q}\nu}$'s except for $\lambda_{M\nu_1}$ decrease with increasing pressure, as shown in Fig. 4(b). Note that even $\lambda_{R\nu_1}$, having the largest

$\langle|D_{\mathbf{q}\nu}|^2\rangle/M_I$, becomes reduced. By contrast, $\lambda_{M\nu_1}$ becomes enhanced because $\omega_{M\nu_1}$ approaches toward zero with increasing pressure, despite the decreasing $N(E_F)$. Namely, the increase of λ_{tot} in pressurized LuPd₂In is caused mainly by the soft phonon mode and the increased $\langle|D_{\mathbf{q}\nu}|^2\rangle/M_I$ at $\mathbf{q} = M$.

Let us discuss the pressure-induced CDW transition in LuPd₂In. As shown in the Supplemental Material [32], the renormalized phonon frequency $\omega_{\mathbf{q}\nu}$ is obtained from the pole of the phonon Green's function,

$$\omega_{\mathbf{q}\nu}^2 = \Omega_{\mathbf{q}\nu}^2 - \left(\frac{\langle|D_{\mathbf{q}\nu}|^2\rangle}{M_I} \right) \chi_{\mathbf{q}}, \quad (1)$$

where $\Omega_{\mathbf{q}\nu}$ is the bare phonon frequency. The imaginary phonon frequency, signifying the CDW instability, occurs when the second term on the right-hand side in Eq. (1) is larger than the first term. Figure 4(d) shows the estimated second term on the right-hand side of Eq. (1). While $\langle|D_{\mathbf{q}\nu}|^2\rangle\chi_{\mathbf{q}}/M_I$ at X and Γ are almost constant, those at M and R increase substantially with increasing pressure, despite the suppression of $\chi_{\mathbf{q}}$. Note that the increasing rate of $\langle|D_{\mathbf{q}\nu}|^2\rangle\chi_{\mathbf{q}}/M_I$ with pressure at M is larger than that at R . Although we do not directly determine the bare phonon-frequency square ($\Omega_{\mathbf{q}\nu}^2$) in the DFT, we can estimate it from Eq. (1) with the calculated $\omega_{\mathbf{q}\nu}^2$ in Fig. 2 and the obtained $\langle|D_{\mathbf{q}\nu}|^2\rangle\chi_{\mathbf{q}}/M_I$ in Fig. 4(d). The estimated $\Omega_{M\nu_1}^2$ (23.2 meV²) turns out to be much smaller than $\Omega_{R\nu_1}^2$ (57.1 meV²), by 2.5 times at the ambient pressure. In general, $\Omega_{\mathbf{q}\nu}^2$ values increase with increasing pressure due to the increment of bonding strength, and it is expected that the difference between $\Omega_{M\nu_1}^2$ and $\Omega_{R\nu_1}^2$ is maintained. Then we can conjecture that the relatively small $\Omega_{M\nu_1}^2$ value and the rapidly increasing $|D_{\mathbf{q}\nu}|^2\chi_{\mathbf{q}}/M_I$ with pressure produce the phonon softening at $\mathbf{q} = M$, which induces the CDW transition in pressurized LuPd₂In above $P \approx 28$ GPa.

Figure 4(e) shows the variation of bond lengths for the nearest-neighbor (NN) Pd-Lu/In and the next-NN Pd-Pd with increasing pressure. Both bond lengths monotonically decrease with increasing pressure. It is noteworthy that, above $P_C \approx 28$ GPa of the CDW transition, both Pd-Pd and Pd-Lu/In bond lengths are split due to the emergence of the CDW phase, suggesting that the splitting size can be taken as the CDW order parameter. Indeed, it is seen in Fig. 4(e) that this order parameter increases continuously with increasing pressure, implying the second-order phase transition [19,42,43]. The splitting increases with pressure, which in turn enhances the rotation of Pd cubes.

The unit cell of the CDW-distorted structure has $\sqrt{2} \times \sqrt{2} \times 1$ of original unit cell with the axes rotated by 45° (see Fig. S1 in the Supplemental Material [32].) Interestingly, the CDW structure of LuPd₂In is identical to that of LuPt₂In [44]. The energy gain in the CDW structure is 0.02 meV/f.u. at $P = 35.7$ GPa. The energy gain increases up to 1.67 meV/f.u. at $P = 69.1$ GPa, as shown

in Fig. 4(f). This result indicates that the CDW state in LuPd₂In becomes more and more stable with increasing pressure. We have checked whether the superconductivity survives in the CDW phase of LuPd₂In. Because of very large unit cell of the CDW state, phonon calculations require heavy computational cost, and so we evaluated λ at only Γ point [45]. We obtained $T_C = 1.18$ K with $\lambda = 0.557$ in the CDW state at $P = 48$ GPa. This result suggests that the SC state and the CDW state would coexist in the high-pressure CDW phase of LuPd₂In, as shown in Fig. 4(f). Because of the suppression of DOS at E_F at the elevated pressure, the SC state in the CDW phase will eventually be suppressed with increasing pressure, which gives rise to a SC-dome feature in Fig. 4(f).

In conclusion, we have found the unusual pressure-induced quantum phase transition to a CDW state with the QCP under the SC dome in LuPd₂In. We have demonstrated that this abnormal transition originates from the extraordinary softened phonon mode at the special $\mathbf{q} = M$, which first enhances λ_{tot} and T_C , but eventually yields the phonon softening instability so as to induce the CDW transition. We have predicted that the CDW QCP can be realized in LuPd₂In by applying pressure of $P \approx 28$ GPa. Experimental verifications of phonon softening at $\mathbf{q} = M$ and the pressure-induced CDW instability in LuPd₂In are urgently demanded to corroborate the underlying physics of unusual CDW QCP, observed in rare-earth-based full-Heusler compound Lu(Pt_{1-x}Pd_x)₂In.

This work was supported by the National Research Foundation (NRF) Korea (Grants No. 2016R1D1A1B02008461, No. 2017R1A2B4005175, No. 2017M2A2A6A01071297, No. 2019R1F1A1052026), Max-Planck POSTECH/KOREA Research Initiative, Study for Nano Scale Optomaterials and Complex Phase Materials (No. 2016K1A4A4A01922028), Internal R&D program at KAERI funded by the MSIT of Korea (No. 524210-20), and KISTI (Grant No. KSC-2017-C2-0042).

*kyoo@kaeri.re.kr

†bimin@postech.ac.kr

- [1] C. W. Chu and L. R. Testardi, Direct Observation of Enhanced Lattice Stability in V₃Si under Hydrostatic Pressure, *Phys. Rev. Lett.* **32**, 766 (1974).
- [2] C. W. Chu, Pressure-Enhanced Lattice Transformation in Nb₃Sn Single Crystal, *Phys. Rev. Lett.* **33**, 1283 (1974).
- [3] L. E. Klintberg, S. K. Goh, P. L. Alireza, P. J. Saines, D. A. Tompsett, P. W. Logg, J. Yang, B. Chen, K. Yoshimura, and F. M. Grosche, Pressure- and Composition-Induced Structural Quantum Phase Transition in the Cubic Superconductor (Sr, Ca)₃Ir₄Sn₁₃, *Phys. Rev. Lett.* **109**, 237008 (2012).
- [4] S. K. Goh, D. A. Tompsett, P. J. Saines, H. C. Chang, T. Matsumoto, M. Imai, K. Yoshimura, and F. M. Grosche, Ambient Pressure Structural Quantum Critical Point in the Phase Diagram of (Ca_xSr_{1-x})₃Rh₄Sn₁₃, *Phys. Rev. Lett.* **114**, 097002 (2015).
- [5] Y. J. Hu, Y. W. Cheung, W. C. Yu, M. Imai, H. Kanagawa, J. Murakawa, K. Yoshimura, and S. K. Goh, Soft phonon modes in the vicinity of the structural quantum critical point, *Phys. Rev. B* **95**, 155142 (2017).
- [6] Y. W. Cheung, Y. J. Hu, M. Imai, Y. Tanioku, H. Kanagawa, J. Murakawa, K. Moriyama, W. Zhang, K. T. Lai, K. Yoshimura, F. M. Grosche, K. Kaneko, S. Tsutsui, and S. K. Goh, Evidence of a structural quantum critical point in (Ca_xSr_{1-x})₃Rh₄Sn₁₃ from a lattice dynamics study, *Phys. Rev. B* **98**, 161103(R) (2018).
- [7] J. J. Yang, Y. J. Choi, Y. S. Oh, A. Hogan, Y. Horibe, K. Kim, B. I. Min, and S.-W. Cheong, Charge-Orbital Density Wave and Superconductivity in the Strong Spin-Orbit Coupled IrTe₂:Pd, *Phys. Rev. Lett.* **108**, 116402 (2012).
- [8] S. Pyon, K. Kudo, and M. Nohara, Superconductivity induced by bond breaking in the triangular lattice of IrTe₂, *J. Phys. Soc. Jpn.* **81**, 053701 (2012).
- [9] K. Kudo, H. Ishii, and M. Nohara, Composition-induced structural instability and strong-coupling superconductivity in Au_{1-x}Pd_xTe₂, *Phys. Rev. B* **93**, 140505(R) (2016).
- [10] C. Heil, S. Ponc e, H. Lambert, M. Schlipf, E. R. Margine, and F. Giustino, Origin of Superconductivity and Latent Charge Density Wave in NbS₂, *Phys. Rev. Lett.* **119**, 087003 (2017).
- [11] D. C. Freitas, P. Rodi re, M. R. Osorio, E. Navarro-Moratalla, N. M. Nemes, V. G. Tissen, L. Cario, E. Coronado, M. Garc a-Hern andez, S. Vieira, M. N u ez-Regueiro, and H. Suderow, Strong enhancement of superconductivity at high pressures within the charge-density-wave states of 2H-TaS₂ and 2H-TaSe₂, *Phys. Rev. B* **93**, 184512 (2016).
- [12] A. F. Kusmartseva, B. Sipos, H. Berger, L. Forr o, and E. Tuti s, Pressure Induced Superconductivity in Pristine 1T-TiSe₂, *Phys. Rev. Lett.* **103**, 236401 (2009).
- [13] C. Pfleiderer, Superconducting phases of f-electron compounds, *Rev. Mod. Phys.* **81**, 1551 (2009).
- [14] S. Nakatsuji, K. Kuga, Y. Machida, T. Tayama, T. Sakakibara, Y. Karaki, H. Ishimoto, S. Yonezawa, Y. Maeno, E. Pearson, G. G. Lonzarich, Balicas, H. Lee, and Z. Fisk, Superconductivity and quantum criticality in the heavy-fermion system β -YbAlB₄, *Nat. Phys.* **4**, 603 (2008).
- [15] J. F. Landaeta, D. Subero, D. Catal a, S. V. Taylor, N. Kimura, R. Settai, Y. Onuki, M. Sigrist, and I. Bonalde, Unconventional superconductivity and quantum criticality in the heavy fermions CeIrSi₃ and CeRhSi₃, *Phys. Rev. B* **97**, 104513 (2018).
- [16] G. R. Stewart, Superconductivity in iron compounds, *Rev. Mod. Phys.* **83**, 1589 (2011).
- [17] J. K. Dong, S. Y. Zhou, T. Y. Guan, H. Zhang, Y. F. Dai, X. Qiu, X. F. Wang, Y. He, X. H. Chen, and S. Y. Li, Quantum Criticality and Nodal Superconductivity in the FeAs-Based Superconductor KFe₂As₂, *Phys. Rev. Lett.* **104**, 087005 (2010).
- [18] H.-H. Kuo, J.-H. Chu, J. C. Palmstrom, S. A. Kivelson, and I. R. Fisher, Ubiquitous signatures of nematic quantum criticality in optimally doped Fe-based superconductors, *Science* **352**, 958 (2016).

- [19] T. Shibauchi, A. Carrington, and Y. Matsuda, A quantum critical point lying beneath the superconducting dome in iron pnictides, *Annu. Rev. Condens. Matter Phys.* **5**, 113 (2014).
- [20] E. Abrahams and Q. Si, Quantum criticality in the iron pnictides and chalcogenides, *J. Phys. Condens. Matter* **23**, 223201 (2011).
- [21] S. Jiang, H. Xing, G. Xuan, C. Wang, Z. Ren, C. Feng, J. Dai, Z. Xu, and G. Cao, Superconductivity up to 30 K in the vicinity of the quantum critical point in $\text{BaFe}_2(\text{As}_{1-x}\text{P}_x)_2$, *J. Phys. Condens. Matter* **21**, 382203 (2009).
- [22] T. Valla, A. Fedorov, P. Johnson, B. Wells, S. Hulbert, Q. Li, G. Gu, and N. Koshizuka, Evidence for quantum critical behavior in the optimally doped cuprate $\text{Bi}_2\text{Sr}_2\text{CaCu}_2\text{O}_{8+\delta}$, *Science* **285**, 2110 (1999).
- [23] S. E. Sebastian, N. Harrison, M. M. Altarawneh, C. H. Mielke, R. Liang, D. A. Bonn, and G. G. Lonzarich, Metal-insulator quantum critical point beneath the high T_C superconducting dome, *Proc. Natl. Acad. Sci. U.S.A.* **107**, 6175 (2010).
- [24] S. Sachdev, Where is the quantum critical point in the cuprate superconductors?, *Phys. Status Solidi* **247**, 537 (2010).
- [25] T. Sarkar, P. R. Mandal, N. R. Poniatowski, M. K. Chan, and R. L. Greene, Correlation between scale-invariant normal-state resistivity and superconductivity in an electron-doped cuprate, *Sci. Adv.* **5**, eaav6753 (2019).
- [26] B. Michon, C. Girod, S. Badoux, J. Kamark, Q. Ma, M. Dragomir, H. A. Dabkowska, B. D. Gaulin, J. S. Zhou, S. Pyon, T. Takayama, H. Takagi, S. Verret, N. Doiron-Leyraud, C. Marcenat, L. Taillefer, and T. Klein, Thermodynamic signatures of quantum criticality in cuprate superconductors, *Nature (London)* **567**, 218 (2019).
- [27] M. Monteverde, J. Lorenzana, P. Monceau, and M. Núñez-Regueiro, Quantum critical point and superconducting dome in the pressure phase diagram of $o\text{-TaS}_3$, *Phys. Rev. B* **88**, 180504(R) (2013).
- [28] T. Gruner, D. Jang, Z. Huesges, R. Cardoso-Gil, G. Fecher, M. Koza, O. Stockert, A. Mackenzie, M. Brando, and C. Geibel, Charge density wave quantum critical point with strong enhancement of superconductivity, *Nat. Phys.* **13**, 967 (2017).
- [29] P. Blaha, K. Schwarz, G. K. H. Madsen, D. Kvasnicka, and J. Luitz, *WIEN2k* (Karlheinz Schwarz, Technische Universität Wien, Austria, 2001).
- [30] S. Baroni, S. de Gironcoli, A. Dal Corso, and P. Giannozzi, Phonons and related crystal properties from density-functional perturbation theory, *Rev. Mod. Phys.* **73**, 515 (2001).
- [31] P. Giannozzi, S. Baroni, N. Bonini, M. Calandra, R. Car, C. Cavazzoni, D. Ceresoli, G. L. Chiarotti, M. Cococcioni, I. Dabo *et al.*, QUANTUM ESPRESSO: A modular and open-source software project for quantum simulations of materials, *J. Phys. Condens. Matter* **21**, 395502 (2009).
- [32] See Supplemental Material at <http://link.aps.org/supplemental/10.1103/PhysRevLett.125.157001> for (i) the computational details, (ii) McMillan's formula, (iii) the deformation potential, (iv) CDW-distorted structure and charge density, and (v) the band structures and DOS of the CDW-distorted phase of LuPd_2In , which includes Refs. [28–31,33–40].
- [33] K. Parlinski, Z. Q. Li, and Y. Kawazoe, First-Principles Determination of the Soft Mode in Cubic ZrO_2 , *Phys. Rev. Lett.* **78**, 4063 (1997).
- [34] W. L. McMillan, Transition temperature of strong-coupled superconductors, *Phys. Rev.* **167**, 331 (1968).
- [35] P. B. Allen and R. C. Dynes, Transition temperature of strong-coupled superconductors reanalyzed, *Phys. Rev. B* **12**, 905 (1975).
- [36] A. Dal Corso, Pseudopotentials periodic table: From H to Pu, *Comput. Mater. Sci.* **95**, 337 (2014).
- [37] D. J. Kim, An itinerant electron model for the critical sound propagation in ferromagnetic metals, *J. Phys. Soc. Jpn.* **40**, 1250 (1976).
- [38] E. G. Maksimov, A self-consistent description of the electron-phonon system in metals and the problem of lattice stability, *Zh. Eksp. Teor. Fiz.* **69**, 2236 (1975).
- [39] G. D. Mahan, *Many-Particle Physics* (Kluwer Academic/Plenum Publishers, New York, 2000).
- [40] F. Giustino, Electron-phonon interactions from first principles, *Rev. Mod. Phys.* **89**, 015003 (2017).
- [41] J. Ying, H. Paudyal, C. Heil, X. Chen, V. V. Struzhkin, and E. R. Margine, Unusual Pressure-Induced Periodic Lattice Distortion in SnSe_2 , *Phys. Rev. Lett.* **121**, 027003 (2018).
- [42] M. A. Continentino and A. S. Ferreira, First-order quantum phase transitions, *J. Magn. Magn. Mater.* **310**, 828 (2007).
- [43] C. Pfleiderer, Why first order quantum phase transitions are interesting, *J. Phys. Condens. Matter* **17**, S987 (2005).
- [44] H. Kim, B. I. Min, and K. Kim, Charge density wave in LuP_2In ($\text{P} = \text{Pt, Pd}$) induced by electron-phonon interaction, *Phys. Rev. B* **98**, 144305 (2018).
- [45] T_C and λ in the CDW state were obtained at only Γ point with the $3 \times 3 \times 3$ k -mesh in the BZ.